J. Meseguer

Axisymmetric Long Liquid Bridges in a Time-Dependent Microgravity Field

This paper deals with the dynamics of liquid bridges when subjected to an oscillatory microgravity field. The analysis has been performed by using a one-dimensional slice model, already used in liquid bridge problems, which allows to calculate not only the resonance frequencies of a wide range of such fluid configurations but also the dependence of the dynamic response of the liquid bridge on the frequency on the imposed perturbations. Theoretical results are compared with experimental ones obtained aboard Spacelab-D1, the agreement between theoretical and experimental results being satisfactory.

1 Introduction

A liquid bridge is an idealization of the fluid configuration appearing in the crystal growth technique known as floating zone melting. The liquid bridge configuration, as sketched in Fig. 1, consists of a mass of liquid held by surface tension forces between two parallel, coaxial, solid disks. Many mechanical aspects of the liquid bridge problem have been extensively studied either from a theoretical or an experimental point of view; a short review of the state of art of theoretical analyses can be found in [1] whereas experimental results have been obtained from experiments performed in Earth-based laboratories [1, 2, 3, 4, 5], aboard TEXUS sounding rockets [6], and in space platforms like Spacelab-1 [7] and Spacelab-D1 [8, 9, 10, 11]. Concerning this last Spacelab Mission, and experiment (WL-FPM-04, Floating Liquid Zones, FLIZ), dealing with the behaviour of long liquid bridges under mechanical disturbances in a low gravity enviroment, was carried out by the German payload specialist *Dr. R. Furrer*. The nominal experiment sequence envisaged consists of liquid injection, disk vibration and rotation of both disks. The overall performance of this experiment was excellent and most of the experimental results obtained have been reported elsewhere [9, 10, 11]. A peculiar aspect observed during FLIZ experiment was that the effect of g-jitter was much higher than in Spacelab-1. In spite of the fact that the Payload Specialist asked for the other crew-members to keep quiet and was granted from the Shuttle pilot a no-maneuvers period, the long columns achieved in Spacelab-D1 were trembling, which, besides the handling problems, has provided valuable information on the behaviour of the liquid bridge when subjected to random perturbations.

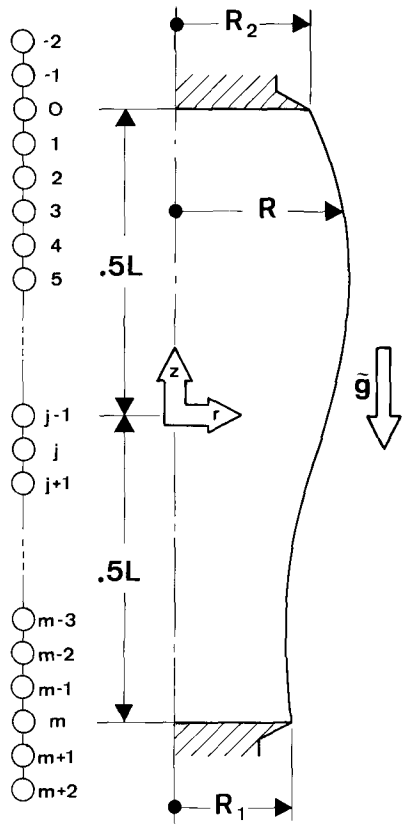

Fig. 1. Geometry and coordinate system for the liquid bridge problem. In this plot a sketch of the spatial grid used in computations is also shown

In this paper a theoretical model for the response of axisymmetric long liquid bridges in an oscillatory axial microgravity field is presented. Although several studies related to the vibration of liquid bridges have been published [3, 12, 13, 14, 15], these studies concern mainly with cylindrical or near cylindrical volume liquid bridges, while the model here presented accounts for effects like liquid volume far from the cylindrical one, different disks radius and a mean level of microgravity added to the oscillatory perturbation. In addition the model allows to calculate not only resonance frequencies of such liquid configurations but also the frequency response of the liquid bridge under such kind of perturbation. Finally, theoretical results are compared with those measured form the FLIZ experiment data.

In the following, unless otherwise stated, all physical quantities are made dimensionless using the characteristic length $R_o=(R_1+R_2)/2$ and the characteristic time

$(\rho R_o^3/\sigma)^{1/2}$, ρ being the liquid density and σ the surface tension.

2 Mathematical Model

Let $S(z)=R^2(z)$ be the dimensionless equation of the liquid-gas interface at rest. Since the problem is assumed to be axisymmetric $S(z)$ will be a solution of

$$P_o = 4\,(4S+S_z^2)^{-3/2}\,(2S+S_z^2-SS_{zz}) + B_o\,z, \tag{1}$$

where P_o is a constant related to the origin of pressures. Terms between parenthesis stand for the capillary pressure and B_o is the Bond number, which measures the steady microgravitational effects, $B_o=\rho g_o R_o^2/\sigma$, g_o being the steady microgravity level. In the following it is assumed that the time variation of microgravity can be expressed as $\tilde{g}(t)=g_o+\varepsilon g(t)$, $\varepsilon \ll 1$, then $B(t)=B_o+\varepsilon b(t)$. Such dependence on time of Bond number will affect the shape of the liquid bridge interface in such a way that the actual shape could be expressed as

$$\tilde{S}(z,t)=S(z)+\varepsilon s(z,t). \tag{2}$$

To analyze the dynamics of the liquid bridge we assume the liquid bridge slenderness $\Lambda=L/(2R_o)$ to be large enough; say $\Lambda>1.5$. In such case the dynamic behaviour of the liquid bridge can be satisfactorily explained by using one-dimensional models like the slice one, widely used in liquid bridge problems [1, 3, 9, 13, 16, 17].

The slice model is based on a one-dimensional theory similar to the one used by *Lee* [18] in the study of the dynamics of capillary jets. The main simplifications introduced by the slice model is that the axial velocity depends only upon the axial coordinate z and the time t. Under that assumption the set of nondimensional differential equations and boundary conditions for the axisymmetric, non-rotating inviscid flow in cylindrical coordinates are drastically reduced [16]. Since the axial velocity does not depend on the radial coordinate, the radial momentum equation becomes decoupled from the other equations and the study of the evolution of the liquid bridge may be accomplished by solving only the continuity equation and the axial momentum equation, i.e.:

$$\tilde{S}_t+\tilde{Q}_z=0, \tag{3}$$

$$\tilde{Q}_t+(\tilde{Q}^2/\tilde{S})_z=-\tilde{S}\tilde{P}_z, \tag{4}$$

where $\tilde{Q}=\tilde{S}\tilde{W}$, $\tilde{W}$ being the axial velocity which, as already stated, is assumed to be constant at each plane parallel to the disks (slice), and

$$\tilde{P}=4\,(4\tilde{S}+\tilde{S}_z^2)^{-3/2}\,(2\tilde{S}+\tilde{S}_z^2-\tilde{S}\tilde{S}_{zz}) + \tilde{B}z. \tag{5}$$

The problem formulation must be completed with boundary conditions at the disks (the liquid bridge remains anchored to the edge of the disks)

$$\tilde{S}(\pm\Lambda,t)=(1\pm H)^2,\ \tilde{Q}(\pm\Lambda,t)=0, \tag{6}$$

where $H=(1-K)/(1+K)$, $K=R_1/R_2$, plus suitable initial conditions.

Since the variables involved in the problem may be rewritten as

$$\left.\begin{aligned}\tilde{S}(z,t)&=S(z)+\varepsilon s(z,t)\\ \tilde{Q}(z,t)&=\varepsilon q(z,t)\\ \tilde{P}(z,t)&=P_o+\varepsilon p(z,t)\\ \tilde{B}(t)&=B_o+\varepsilon b(t)\end{aligned}\right\} \tag{7}$$

after substituting these expressions in (3)-(6), leaving appart ε^2 terms, there results

$$s_t+q_z=0, \tag{8}$$

$$q_t=-Sp_z, \tag{9}$$

$$s(\pm\Lambda,t)=0,\ q(\pm\Lambda,t)=0. \tag{10}$$

Note that both terms in the product Sp_z in equation (9) depend on the unperturbed equilibrium interface shape $S(z)$ (see the Appendix for the expression of $p(z,t)$).

To solve the problem a procedure similar to that used in [16] has been employed, eliminating the variable s between (8) and (9). Differentiation of (9) with respect to time gives

$$q_{tt}=-Sp_{zt}, \tag{11}$$

and differentiation of continuity equation (8) with respect to z as many times as necessary yields

$$s_{zt}=-q_{zz},\ s_{zzt}=-q_{zzz},\ \ldots. \tag{12}$$

which allows us to eliminate the variable s and its derivatives appearing in the term p_{zt} of equation (11). Then

$$\begin{aligned}q_{tt}=-Sp_{zt}=-S\{&4A^{-3/2}\,[(6D/A-4-S_{zz})s_t+\\ &(3D/A-1)S_z s_{zt}-Ss_{zzt}]\}_z-Sb_t=S\{4A^{-3/2}\,[(6D/A-4-S_{zz})q_z+\\ &(3D/A-1)S_z q_{zz}-Sq_{zzz}]\}_z-Sb_t.\end{aligned} \tag{13}$$

The boundary conditions are

$$q(\pm\Lambda,t)=0,\ q_z(\pm\Lambda,t)=0, \tag{14}$$

where the second of these conditions results from $s(\pm\Lambda,t)=0$, taking into account equation (8). Functions A and D are shown in the Appendix and in expressions (24) and (25) of this section.

Assuming the Bond number dependence on time is

$$b=\beta\sin\omega t, \tag{15}$$

equation (13) suggests to look for $q(z,t)$ solutions of the form

$$q=u(z)\cos\omega t \tag{16}$$

Therefore, after substituting (16) in (13), and eliminating time dependent factors, there results

$$\begin{aligned}&\omega^2 u+S\{4A^{-3/2}\,[(6D/A-4-S_{zz})u_z+(3D/A-1)S_z u_{zz}\\ &-Su_{zzz}]\}_z-\beta\omega S=0,\end{aligned} \tag{17}$$

$$u(\pm\Lambda)=0,\ u_z(\pm\Lambda)=0 \tag{18}$$

3 Numerical Solution

Equation (17), once the terms between brackets differentiated, yields

$$Su_{zzzz} + k_3 u_{zzz} + k_2 u_{zz} + k_1 u_z - A^{3/2}\omega^2 u/(4S) = -A^{3/2}\beta\omega/4, \quad (19)$$

$$u(\pm\Lambda) = u_z(\pm\Lambda) = 0, \quad (20)$$

where

$$k_3 = (2 - 3D/A)S_z - 3SA_z/(2A), \quad (21)$$

$$k_2 = (3D/A - 1)[3S_z A_z/(2A) - S_{zz}] - 6D/A + S_{zz} + 4 - 3(AD_z - DA_z)S_z/A^2, \quad (22)$$

$$k_1 = 3(6D/A - S_{zz} - 4)A_z/(2A) - 6(AD_z - DA_z)/A^2 + S_{zz}, \quad (23)$$

and

$$A = 4S + S_z^2, \quad A_z = 2S_z(2 + S_{zz}), \quad (24)$$

$$D = S(2 + S_{zz}), \quad D_z = S_z(2 + S_{zz}) + SS_{zzz}. \quad (25)$$

To solve (19) an implicit finite-difference method has been used, with a centered five-point scheme for the evaluation of the spatial derivatives

$$\begin{aligned}
(u_z)_j &= [8(u_{j+1} - u_{j-1}) - u_{j+2} + u_{j-2}]/(12\Delta) \\
(u_{zz})_j &= [16(u_{j+1} + u_{j-1}) - u_{j+2} - u_{j-2} - 30u_j]/(12\Delta^2) \\
(u_{zzz})_j &= [-2(u_{j+1} - u_{j-1}) + u_{j+2} - u_{j-2}]/(2\Delta^3) \\
(u_{zzzz})_j &= [-4(u_{j+1} + u_{j-1}) + u_{j+2} + u_{j-2} + 6u_j]/(\Delta^4)
\end{aligned} \quad (26)$$

where $\Delta = 2\Lambda/m$, m being the number of equally spaced steps used in the numerical integration (see Fig. 1). Substitution of expressions (26) in (19) gives

$$C_{-2,j}u_{j-2} + C_{-1,j}u_{j-1} + C_{0,j}u_j + C_{1,j}u_{j+1} + C_{2,j}u_{j+2} = -(A_j)^{3/2}\beta\omega/4, \quad (27)$$

with $0 \le j \le m$, and

$$C_{2i,j} = [S_j/\Delta^2 - (k_2)_j/12]/\Delta^2 + \mathrm{sgn}(i)[(k_3)_j/(2\Delta^2) - (k_1)_j/12]/\Delta, \quad (28)$$

$$C_{i,j} = [-4S_j/\Delta^2 + 4(k_2)_j/3]/\Delta^2 + \mathrm{sgn}(i)[-(k_3)_j/\Delta^2 - 2(k_1)_j/3]/\Delta, \quad (29)$$

$$C_{0,j} = [6S_j/\Delta^2 - 5(k_2)_j/2]/\Delta^2 - (A_j)^{3/2}\omega^2/(4S_j), \quad (30)$$

in these last expressions the subscript i has two possible values, 1 or -1, and the function sgn (i) stands for the sign of i.

Boundary conditions (see Fig. 1) are

$$\left.\begin{aligned}
&u(-\Lambda) = 0 \rightarrow u_0 = 0 \\
&u(\Lambda) = 0 \rightarrow u_m = 0 \\
&u_z(-\Lambda) = 0 \rightarrow u_{-2} - 8u_{-1} + 8u_1 - u_2 = 0 \\
&u_z(\Lambda) = 0 \rightarrow u_{m-2} - 8u_{m-1} + 8u_{m+1} - u_{m+2} = 0
\end{aligned}\right\} \quad (31)$$

Therefore, there are m+3 unknowns: $m-1$ unknows come from the liquid bridge (remember that $u_0 = 0$ $u_m = 0$) and the four remainder correspond to the outher points needed to meet boundary conditions. On the other hand, there are $m+3$ equations, $m+1$ result from expression (27) plus the two last of (31). In conclusion, the system to be solved results in (32) (see below):

where $T_j = -(A_j)^{3/2}\beta\omega/4$. Equation (32) can be written in a more compact form as

$$[M]\cdot[U] = [T], \quad (33)$$

so that the problem solution becomes

$$[U] = [M]^{-1}[T]. \quad (34)$$

Resonance frequencies are obtained from those values of ω for which the determinant of the matrix $[M]$ vanishes, $|M| = 0$. In addition, once $[U]$ is known, equation (16) gives $q(z,t)$, and the continuity equation (8) allows to calculate $s(z,t)$ from $q(z,t)$.

Obviously, a previous step needed to calculate $[M]$ and $[T]$ is to determine the unperturbed liquid bridge interface $S(z)$, which depends on the liquid volume V, slenderness Λ, disks radius ratio K, and Bond number B_0. A description of the procedure used to calculate $S(z)$ can be found in [19].

4 Results

Before the results obtained are presented, it would be convenient to make some comments on the accuracy of the numerical computation. A typical feature of problems where surface-tension effects are present is the high order of the spatial

Equation (32):

$$\begin{bmatrix}
1 & -8 & 8 & -1 & 0 & 0 & 0 & 0 & \dots & 0 & 0 \\
C_{-2,0} & C_{-1,0} & C_{1,0} & C_{2,0} & 0 & 0 & 0 & 0 & \dots & 0 & 0 \\
0 & C_{-2,1} & C_{0,1} & C_{1,1} & C_{2,1} & 0 & 0 & 0 & \dots & 0 & 0 \\
0 & 0 & C_{-1,2} & C_{0,2} & C_{1,2} & C_{2,2} & 0 & 0 & \dots & 0 & 0 \\
0 & 0 & C_{-2,3} & C_{-1,3} & C_{0,3} & C_{1,3} & C_{2,3} & 0 & \dots & 0 & 0 \\
0 & 0 & 0 & C_{-2,4} & C_{-1,4} & C_{0,4} & C_{1,4} & C_{2,4} & \dots & 0 & 0 \\
\dots & \dots & \dots & \dots & \dots & \dots & \dots & \dots & \dots & \dots & \dots \\
\dots & \dots & \dots & \dots & \dots & \dots & \dots & \dots & \dots & \dots & \dots \\
\dots & \dots & \dots & \dots & \dots & \dots & \dots & \dots & \dots & \dots & \dots \\
0 & 0 & \dots & C_{-2,m-4} & C_{-1,m-4} & C_{0,m-4} & C_{1,m-4} & C_{2,m-4} & 0 & 0 & 0 \\
0 & 0 & \dots & 0 & C_{-2,m-3} & C_{-1,m-3} & C_{0,m-3} & C_{1,m-3} & C_{2,m-3} & 0 & 0 \\
0 & 0 & \dots & 0 & 0 & C_{-2,m-2} & C_{-1,m-2} & C_{0,m-2} & C_{1,m-2} & 0 & 0 \\
0 & 0 & \dots & 0 & 0 & 0 & C_{-2,m-1} & C_{-1,m-1} & C_{0,m-1} & C_{2,m-1} & 0 \\
0 & 0 & \dots & 0 & 0 & 0 & 0 & C_{-2,m} & C_{-1,m} & C_{1,m} & C_{2,m} \\
0 & 0 & \dots & 0 & 0 & 0 & 0 & 1 & -8 & 8 & -1
\end{bmatrix}
\begin{bmatrix} u_{-2} \\ u_{-1} \\ u_1 \\ u_2 \\ u_3 \\ u_4 \\ \dots \\ \dots \\ \dots \\ u_{m-4} \\ u_{m-3} \\ u_{m-2} \\ u_{m-1} \\ u_{m+1} \\ u_{m+2} \end{bmatrix}
=
\begin{bmatrix} 0 \\ T_0 \\ T_1 \\ T_2 \\ T_3 \\ T_4 \\ \dots \\ \dots \\ \dots \\ T_{m-4} \\ T_{m-3} \\ T_{m-2} \\ T_{m-1} \\ T_m \\ 0 \end{bmatrix}$$

derivatives involved. In our particular case these derivatives have been calculated through a five-point scheme. Leaving apart the fact that the approximation in numerical evaluation of derivatives decreases as the order of differentiation increases, there is a source of error associated with the five-point scheme used which arises when these derivatives are evaluated close to the boundary points. In effect, this scheme introduces four outer points (two external points at each disk) in which the values of u must be calculated to meet boundary conditions. Since these outer values, which have no physical meaning, affect some terms of the matrix $[M]$, the outer points introduce some spurious information in calculations, whose effect decreases with the size Δ of the spatial grid. Therefore, the first computations have been performed aiming at establishing the optimum of this grid size, running a test case ($\Lambda=2.6$, $V=16.34$, $B_0=0$, $K=1$) several times and varying each time the number of steps m between the disks. The results obtained are plotted in Fig. 2, which shows that the resonance pulsation ω_r increases with m but the rate of increase tends to zero for large values of m (the slope is practically zero at $m=60$). The variation with m of the computation time is also presented in this plot. As it can be observed this computation time increases almost exponentially with m. Therefore, choosing a value for m is a trade-off between accuracy and computing time. For all other computations the value $m=40$ has been used; this value gives, according to Fig. 2, a resonance frequency already 99.7% of that obtained from $m=60$ whereas computing time is more than three times smaller.

The transfer function, defined as the module of the ratio of the maximum interface deformation to the perturbation amplitude, $A=|(s_{max}-s_{min})/\beta|$, for a liquid bridge with $\Lambda=2.6$, $V=16.34$, $K=1$ an $B_0=0$, is shown in Fig. 3. This plot shows a phenomenon already observed aboard Spacelab-1 and Spacelab-D1: the liquid bridge is mainly affected by low frequency perturbations (Except in the vicinity of the resonance frequencies $A(\omega)$ decreases quickly as ω increases. The higher the forcing frequency ω the less deeply the waves

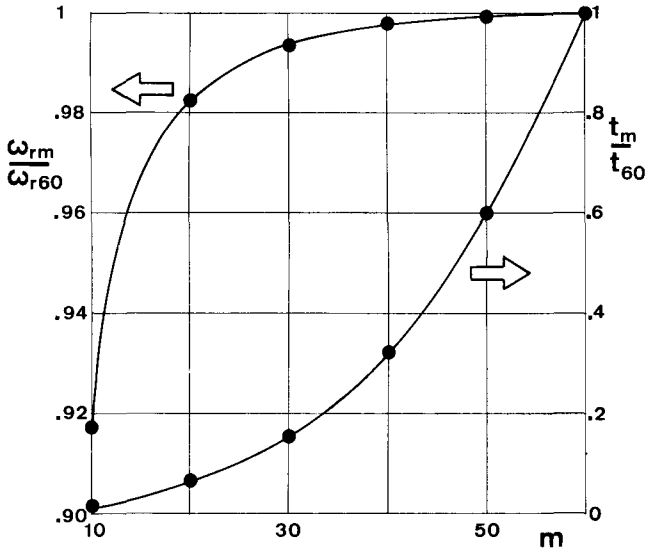

Fig. 2. Variation with the number m of steps of the spatial grid used in computations of the resonance pulsation ω_{rm} and the computation time t_m of a liquid bridge with $\Lambda=2.6$, $V=16.34$, $B_0=0$ and $K=1$

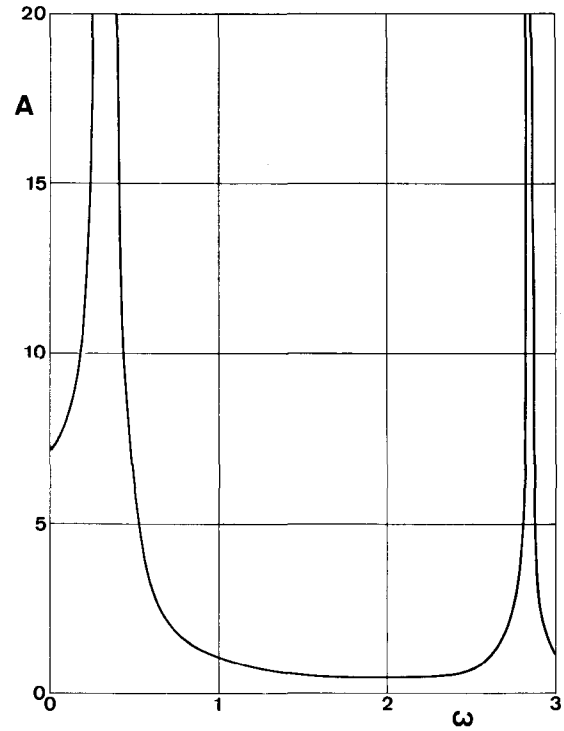

Fig. 3. Transfer function, defined as the variation with the pulsation ω of the module of the ratio of the maximum interface deformation to the perturbation amplitude, $A=|(s_{max}-s_{min})/\beta|$. The results correspond to the case $\Lambda=2.6$, $V=16.34$, $K=1$, $B_0=0$

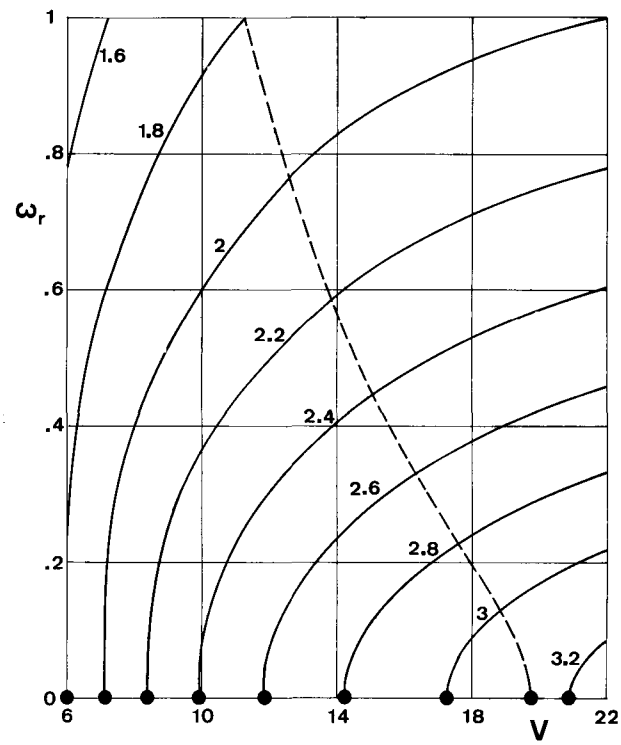

Fig. 4. Variation with the liquid bridge volume V of the pulsation of resonance corresponding to the first mode ω_r of liquid bridges between equal disks ($K=1$) in gravitationless conditions ($B_0=0$). Numbers on the curves indicate the value of the slenderness Λ. The dashed line corresponds to liquid bridges with cylindrical-volume ($V=2\pi\Lambda$)

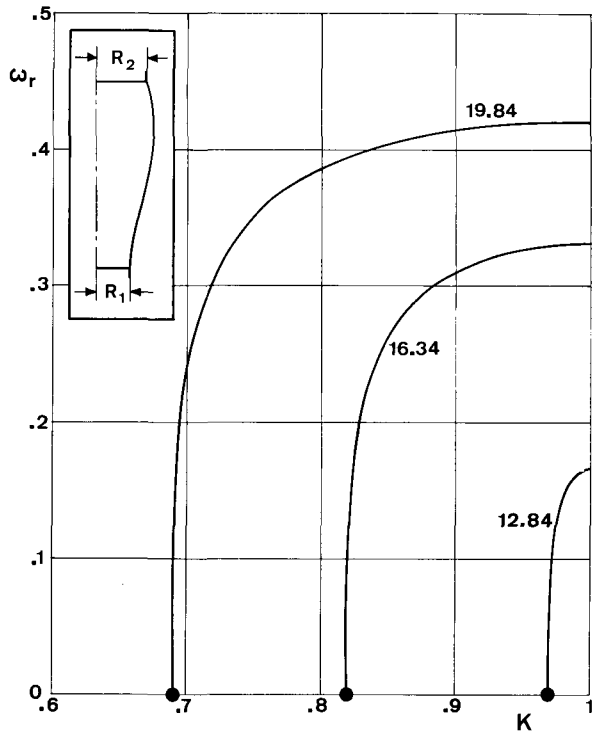

Fig. 5. Influence on the pulsation of resonance ω_r of the disks radius ratio, $K=R_1/R_2$. The results correspond to the case $\Lambda=2.6$, $B_o=0$. Numbers on the curves indicate the value of the volume of the liquid bridge

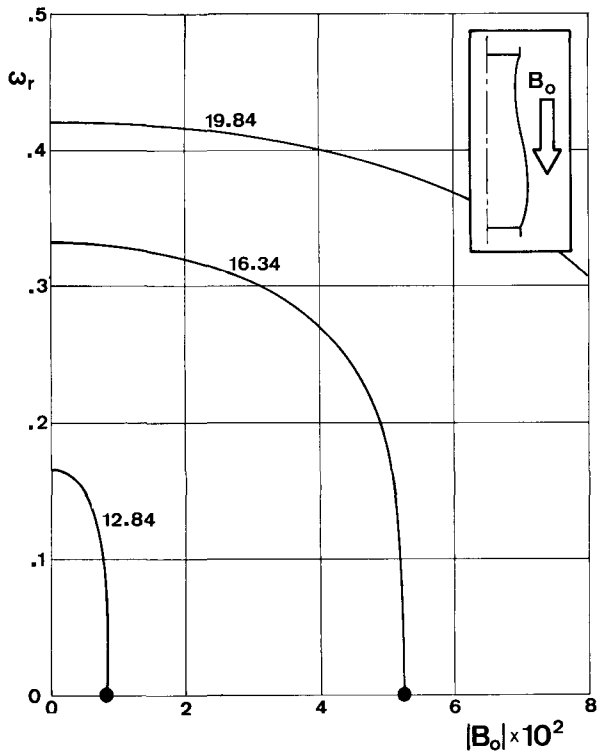

Fig. 6. Influence on the pulsation of resonance ω_r of the steady Bond number, B_o. The results correspond to the case $\Lambda=2.6$, $K=1$. Numbers on the curves indicate the value of the volume of the liquid bridge

on the liquid surface penetrate into the bulk of the liquid and therefore, the surface amplitude decreases considerably for higher modes).

A mapping of fundamental axisymmetric resonance frequencies (first mode) of liquid bridges between equal disks ($K=1$) in a zero mean-value gravitational field ($B_o=0$) is shown in Fig. 4. As one could expect, for each value of the slenderness the value $\omega_r=0$ being reached when the volume becomes that of minimum volume stability limit [19]. The dashed line in this plot corresponds to cylindrical volume liquid bridges ($V=2\pi\Lambda$) whose resonance frequencies are well known, as already indicated in § 1.

The influence on ω_r of K or B_0 is shown in Figs. 5 and 6, respectively. In both cases the behaviour of the liquid bridge becomes similar, as K decreases (or B_0 increases) ω_r becomes smaller, the reason being that the minimum volume stability limit increases as $K \neq 1$ (the same applies when $B_0 \neq 0$, [1, 17, 19]).

Table 1. Dimensionless resonance frequencies ($f=2\pi\omega_r$) of liquid bridges between equal disks ($K=1$) of slenderness Λ and dimensionless volume V, subjected to an axial microgravity field measured by the steady Bond number B_o. The subscript e indicates experimental results obtained from the FLIZ experiment whereas the subscript n indicates numerical ones

Λ	$V \pm 0.05$	B_o	ω_{re}	$\omega_m \pm 0.002$
2.571	16.28	0.009	0.30	0.348
2.714	16.82	0.009	0.23	0.259
2.854	18.84	0.009	0.19	0.222
2.857	17.92	0.010	0.14	0.177

Finally, in Table 1, numerical results are compared with experimental ones obtained from the FLIZ experiment[1]. Experimental results have been obtained from the analysis of some periods of the FLIZ sequence in which the liquid bridge was oscillating in spite of the absence of intentionally imposed perturbations during these periods. Previous studies published elsewhere [20] show that during the four analyzed periods the only perturbation acting on the liquid bridge can be nearly considered as a white noise, so that, in every case, the liquid bridge oscillates with its natural frequency. Comparison of both numerical and experimental results indicate that numerical results are some 20% higher than experimental ones. Therefore, numerical results can be considered good enough if one takes into account that they have been obtained through a linear analysis of a simplified one-dimensional model.

[1] To made dimensionless the experimental results, the following values have been used, $R_0=0.0175$ m, $\rho=920$ kg m^{-3}, $\sigma=0.02$ N m^{-1}.

Appendix

To save typing, let us introduce the functions

$$\tilde{A}=4\tilde{S}+\tilde{S}_z^2,\ A=4S+S_z^2$$

$$\tilde{D}=\tilde{S}(2+\tilde{S}_{zz}),\ D=S(2+S_{zz})$$

so that expression (5) becomes

$$\tilde{P}=4\tilde{A}^{-3/2}(\tilde{A}-\tilde{D})+\tilde{B}z. \qquad \text{(A.1)}$$

Introduction of the asymptotic expansions (7) in the expression for $\tilde{A}$ and $\tilde{D}$ yields:

$$\tilde{A} = 4S + S_z^2 + 2\varepsilon\,(2s + S_z s_z) + O(\varepsilon^2) = A + \varepsilon\, a + O(\varepsilon^2)$$

$$\tilde{D} = S(2 + S_{zz}) + \varepsilon\,[(2 + S_{zz})s + S s_{zz}] + O(\varepsilon^2) = D + \varepsilon d + O(\varepsilon^2)$$

where

$$a = 4S + 2S_z s_z$$

$$d = (2 + S_{zz})s + S s_{zz}$$

Then, expression (A.1) results

$$\tilde{P} = P_0 + \varepsilon p = A^{-3/2}\,[1 + \varepsilon a/A + O(\varepsilon^2)]^{-3/2} \cdot$$

$$\cdot\,[A - D + \varepsilon(a - d) + O(\varepsilon^2)] + B_0 z + \varepsilon b z = 4A^{-3/2}(A - D)$$

$$+ B_0\, z + \varepsilon\{4A^{-3/2}\,[a - d - 3a(A - D)/(2A)] + bz\} + O(\varepsilon^2)$$

Therefore, taking into account that $P_0 = 4A^{-3/2}(A - D) + B_0 z$. and the expressions for a and d..it finally results

$$P = 4A^{-3/2}\,[(6D/A - 4 - S_{zz})s + (3D/A - 1)\,S_z s_z - S s_{zz}] + bz$$

References

1 *Meseguer, J., Sanz, A.:* J. Fluid Mech. 153, 83 (1985).
2 *Sanz, A., Martínez, I.:* J. Colloid Interface Sci. 93, 235 (1983).
3 *Sanz, A.:* J. Fluid Mech. 156, 101 (1985).
4 *Meseguer, J., Mayo, L.A., Llorente, J.C., Fernández, A.:* J. Crystal Growth 73, 609 (1985).
5 *Russo, M.J., Steen, P.H.:* J. Colloid Interface Sci. 113, 154 (1986).
6 *Martínez, I., Sanz, A.:* ESA Journal 9, 323 (1985).
7 *Martínez, I.:* in ESA SP-222, ESA, Paris, p. 31/36 (1984).
8 *Da Riva, I., Martínez, I.:* Naturwissenschaften 73, 345 (1986).
9 *Meseguer, J., Sanz, A., López, J.:* J. Crystal Growth 78, 325 (1986).
10 *Martínez, I.:* Acta Astronautica 15, 449 (1987).
11 *Martínez, I.:* in ESA SP-256, ESA, Paris, p. 235/240 (1987).
12 *Bauer, H.F.:* Acta Astronautica 9, 547 (1982).
13 *Rivas, D., Meseguer, J.:* J. Fluid Mech. 138, 417 (1984).
14 *Bauer, H.F.:* Acta Astronautica 13, 9 (1986).
15 *Langbein, D.:* in ESA SP-256, ESA, Paris, p. 221/228 (1987).
16 *Meseguer, J.:* J. Fluid Mech. 130, 123 (1983).
17 *Meseguer, J.:* J. Crystal Growth 73, 599 (1985).
18 *Lee, H.C.:* IBM J. Res. Develop. 18, 364 (1974).
19 *Martínez, I., Perales, J.M.:* J. Crystal Growth 78, 369 (1986).
20 *Meseguer, J., Sanz, A.:* An. Real Soc. Esp. Fis., in Spanish (in press).